Available online at www.sciencedirect.com
ScienceDirect
Ceramics International 38S (2012) S411–S414
CERAMICS INTERNATIONAL
www.elsevier.com/locate/ceramint

Dielectric properties and related ferroelectric domain configurations in multiferroic $BiFeO_3$–$BaTiO_3$ solid solutions

Qiming Hang [a], Zhibiao Xing [a], Xinhua Zhu [a,*], Miao Yu [a], Ye Song [a], Jianmin Zhu [a], Zhiguo Liu [b]

[a] National Laboratory of Solid State Microstructures, School of Physics, Nanjing University, Nanjing 210093, China
[b] Department of Materials Science and Engineering, National Laboratory of Solid State Microstructures, Nanjing University, Nanjing 210093, China

Available online 12 May 2011

Abstract

Dielectric properties and ferroelectric domain configurations of multiferroic $x BaTiO_3$–$(1-x)BiFeO_3$ ($x = 0.10$–0.33) solid solutions synthesized by conventional solid-state reaction, were reported. A structural transition from rhombohedral to pseudo-cubic structures appeared around $x = 0.33$, and the formation of impurity phase of $Bi_2Fe_4O_9$ was effectively depressed by doping $BaTiO_3$. Dielectric constants of $x BaTiO_3$–$(1-x)BiFeO_3$ solid solutions decreased with increasing the frequency, and the degree of decrease was related to the doping content of $BaTiO_3$. Transmission electron microscopy images revealed that the ferroelectric domain configurations in the multiferroic $BiFeO_3$–$BaTiO_3$ solid solutions with rhombohedral symmetry, exhibited a wavy character whereas a predominant intricate domain structure with fluctuating mottled contrast was observed in the multiferroic $BiFeO_3$–$BaTiO_3$ solid solution with pseudo-cubic phase structure. The presence of 1/2{1 1 1} superlattice spots in the selected area electron diffraction patterns taken from the multiferroic $BiFeO_3$–$BaTiO_3$ solid solutions with rhombohedral symmetry indicated that the ordered regions have a doubled perovskite unit cell.
© 2011 Elsevier Ltd and Techna Group S.r.l. All rights reserved.

Keywords: C. Dielectric properties; $BiFeO_3$–$BaTiO_3$ solid solution; Ferroelectric domain configurations; Multiferroic ceramics

1. Introduction

Multiferroic materials have been received much attention because of their potential applications for new types of electronic devices (e.g., multiple-state memories and new date-storage media) [1,2]. An important number of magnetoelectric muliferroics has the general chemical formula ABO_3 and crystallizes in a perovskite or perovskite-related structure [3]. Perovskite bismuth ferrite $BiFeO_3$ (BFO), as one of the single-phase magnetoelectric multiferroics, it is ferroelectric with the Curie temperature $T_C \approx 830\ ^\circ C$ and antiferromagnetic having the Néel temperature $T_N = 310\ ^\circ C$, therefore, it is an interesting model muliferroics, perhaps the only material that exhibits spontaneous ferroelectric and magnetic ordering above room temperature [2].

However, since the discovery of BFO in the 1960s, difficult synthesis of pure BFO and its large current leakage have hampered its practical applications. Actually, only low values of the polarization and of the dielectric constant were determined at room temperature, mainly due to the semi-conducting properties of BFO, which does not allow proper electrical poling and leads to high dielectric losses. Several techniques such as solid-state reaction, co-precipitation method, and soft chemical route, were used to synthesize pure BFO. Meanwhile, the solid solutions of BFO formed with other ABO_3 perovskites such as $BaTiO_3$ (BTO) and $PbTiO_3$ with good dielectric properties, were also synthesized in order to reduce the leakage current and to achieve high resistivity. Recently, BTO–BFO solid solution has been prepared by classical solid-state reaction method, and their magnetic and dielectric properties were reported [4–6]. However, the problems of dielectric losses in the solid solution of BTO–BFO were only partially solved and the reported data are often ''author dependent''. In the present work, we report on the dielectric properties of perovskite multiferroic xBTO–$(1-x)$BFO

* Corresponding author. Tel.: +86 25 83592772; fax: +86 25 83595535.
E-mail address: xhzhu@nju.edu.cn (X. Zhu).

0272-8842/$36.00 © 2011 Elsevier Ltd and Techna Group S.r.l. All rights reserved.
doi:10.1016/j.ceramint.2011.05.022

($x = 0.1$–0.33) solid solutions synthesized by solid-state reaction. The ferroelectric domain configurations in the multiferroic BTO–BFO solid solutions were also examined by bright- and dark-field transmission electron microscopy (TEM) images and selected area electron diffraction technique.

2. Experimental

The perovskite solid solutions of xBTO–$(1-x)$BFO ($x = 0.10$–0.33) were prepared by a conventional solid-state reaction method. The stoichiometric amounts of starting materials, Bi_2O_3, Fe_2O_3, $BaCO_3$, and TiO_2 were mixed and ball-milled for 24 h in polyethylene container with zirconia balls. After drying at 120 °C, the mixed powders were then calcined at 750 °C for 4 h. Subsequently, the calcined samples were pressed into disc shape and pre-sintered at 820–850 °C for 2 h with intermediate grindings. The crushed powder was then mixed with appropriate amount of polyvinyl alcohol, and then pressed into cylindrical pellets with a diameter of 10 mm and thickness of 1.5 mm. Final sintering temperatures were increased with the increasing content of BTO taking into account the fact that BTO reacts at fairly high temperatures. The samples were finally sintered at between 930 and 945 °C for 1 h. The crystal structures of the sintered pellets were examined by X-ray diffraction (XRD) using CuKα radiation. A typical scan rate was 0.02°/s, and the 2θ range was 10–80°. For electrical properties characterization, the sintered samples were ground to obtain parallel faces, and the two faces were then coated with Ag–Pd paint as electrodes. The dielectric properties of the sintered ceramics were measured as a function of temperature and frequency using a HP4192A impedance analyzer controlled by a computer. Ferroelectric domain configurations were examined by a field-emission TEM (FE-TEM, FEI Tecnai F20) operated at 200 kV. The TEM specimens were prepared from the polycrystalline samples by mechanical grinding, dimple grinding, and subsequently ion-milling.

3. Results and discussion

Fig. 1(a) shows the XRD patterns of xBTO–$(1-x)$BFO ($x = 0.10$–0.33) solid solutions prepared by a conventional solid-state reaction method. The XRD patterns were indexed on the basis of data of BFO (rhombohedral, space group R3c) and showed rhombohedral distortion. A few small traces of impurity were observed in the case of $x = 0.25$–0.33, which were found to be those of $Bi_2Fe_4O_9$ (labeled by a star in Fig. 1(a)). With increasing the concentration of BTO from $x = 0.10$ to 0.33, the (0 0 6)/(2 0 2) diffraction peaks shifted towards the lower angle, as shown in Fig. 1(b) in detail, and the decrease of rhombohedral distortion was also observed, as demonstrated by gradual disappearance of the splitting of the diffraction peaks such as (0 0 6) and (2 0 2) peaks in Fig. 1(b). The lattice parameter (a) and rhombohedral angle (α) as a function of the increase of the BTO concentration were shown in Fig. 2(a), and the change of volume of the unit cell was demonstrated in Fig. 2(b). It was noticed that the rhombohedral angle, α approached to 90° (a specific value to the pseudo-cubic phase) as the concentration of BTO reached $x = 0.33$, and the lattice parameter a increased linearly with the increase of the BTO concentration. Similar phenomenon was also observed in the volume of the unit cell, as shown in Fig. 2(b), which is ascribed to that the ionic radii of Ba^{2+} (135 pm) is much larger than that of Bi^{3+} (108 pm), and also the ionic radii of Ti^{4+}(68 pm) larger than that of Fe^{3+} (64 pm). These results are in agreement the data previously reported by Kumar et al. [4].

Fig. 3 shows the dielectric properties of the BTO–BFO solid solutions as a function of the measured frequency. As shown in Fig. 3(a) the dielectric constants of all the BTO–BFO solid solutions had a general tendency to decrease with increasing the frequency. Such a decrease of the dielectric constant in the low-frequency region below 100 kHz, is caused by space charge polarization, due to the inevitable oxygen vacancies, A-site vacancies, and the Fe^{3+}/Fe^{2+} coexistence in the perovskite BTO–BFO multiferroic ceramics. As observed in Fig. 3, the BTO–BFO solid solution with $x = 0.15$ had much larger dielectric constant as compared to the other solid solutions ($x = 0.20$–0.33) (see Fig. 3(a)), and its dielectric loss ($\tan\delta$) also had a much high value (0.2–0.3) (see Fig. 3(b)). That was attributed to the space charge polarization induced by the structural defects such as oxygen vacancies, A-site vacancies, and the coexistence of Fe^{3+}/Fe^{2+} ions in this solid solution. On the other hand, the dielectric constants of the BTO–BFO solid

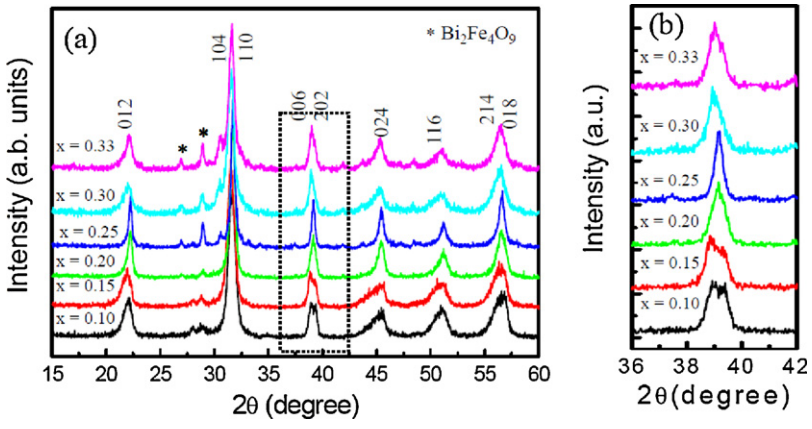

Fig. 1. (a) XRD patterns of xBTO–$(1-x)$BFO solid solutions ($x = 0.10$–0.33) prepared by a solid-state reaction method. (b) Local ($2\theta = 36$–$42°$) XRD patterns. With increasing the concentration (x) of BTO from 0.10 to 0.33, the diffraction peaks (0 0 6) and (2 0 2) shifted towards the lower angle.

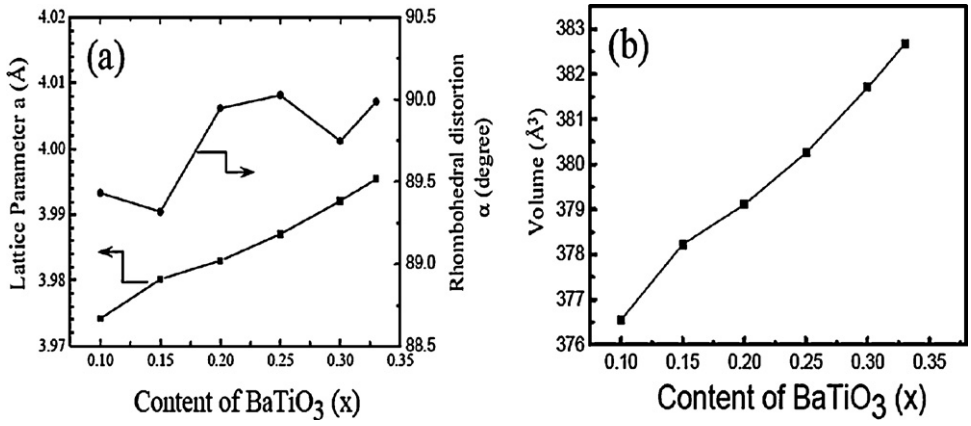

Fig. 2. (a) Lattice parameter (a) and rhombohedral angle (α) as a function of the BTO concentration in the xBTO–$(1-x)$BFO solid solutions. (b) Volume change of the unit cell as a function of the BTO concentration.

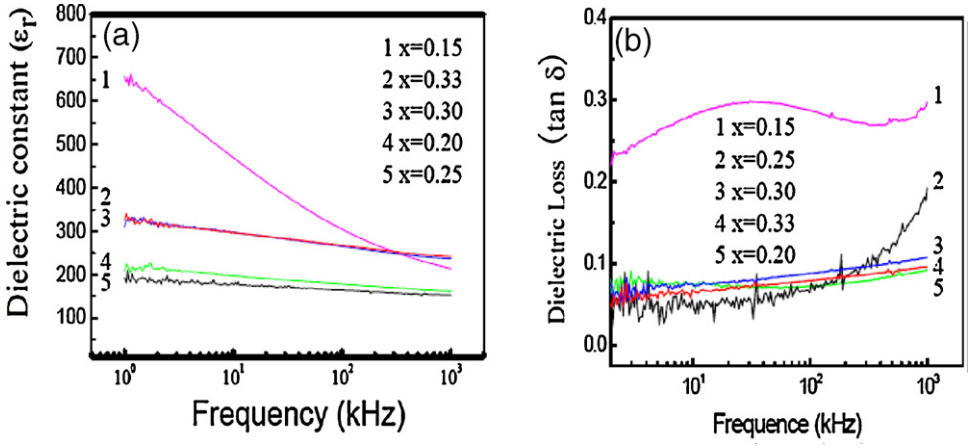

Fig. 3. Frequency dependence of dielectric constant (a) and dielectric loss (b) of the xBTO–$(1-x)$BFO solid solutions ($x = 0.10$–0.33) measured at room temperature.

solutions with $x = 0.20$–0.25, were much reduced as compared to $x = 0.15$, which might be originated from the reduced space charge concentration, and consequently the reduced values of the dielectric losses (see Fig. 3(b)). As further increasing the BTO content ($x = 0.30$–0.33), the increase of the dielectric constant could be ascribed to the larger dielectric constant of BTO (>1000) than the BFO (<150).

The rhombohedral (ferroelectric) domains in BTO–BFO multiferroic ceramics were examined by bright- and dark-field TEM images and SAED techniques. Fig. 4(a) shows the [1$\underline{1}$0] zone axis SAED pattern obtained from the 0.25BTO–0.75BFO multiferroic ceramic sample at room temperature. The diffraction spots in the SAED pattern are indexed based on the basis of the high-temperature cubic Pm3m structure. As

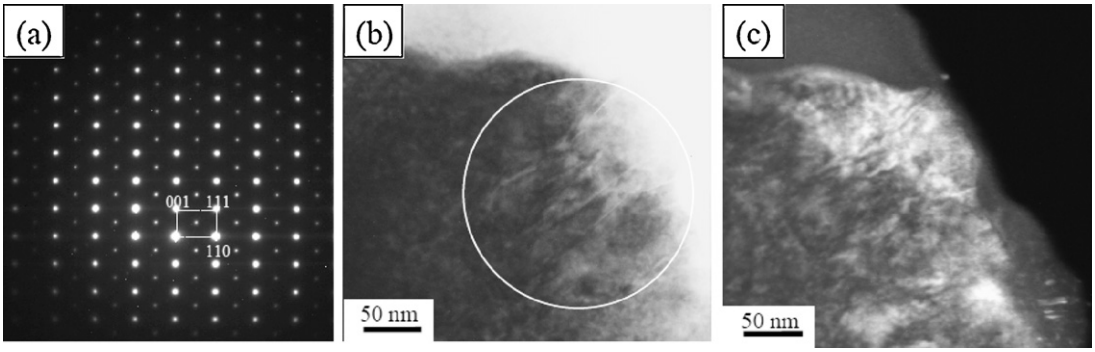

Fig. 4. (a) [1$\underline{1}$0] zone-axis selected area diffraction pattern obtained from the 0.25BTO–0.75BFO solid solution at room temperature. (b and c) Bright- and dark-field TEM images of the ferroelectric domain configurations observed in the 0.25BTO–0.75BFO solid solution with a rhombohedral symmetry. The dark-field TEM image was obtained using the (1 1 0) fundamental spot.

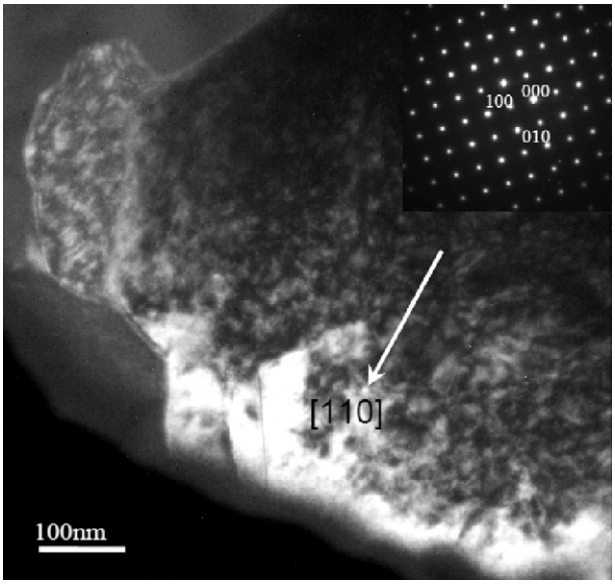

Fig. 5. Dark-field TEM image (obtained by the (1 0 0) diffraction spot) of the ferroelectric domain configurations observed in the 0.33BTO–0.67BFO solid solution with a pseudo-cubic symmetry. The inset is [0 0 1] zone-axis selected area electron diffraction pattern.

shown in the SAED pattern, besides the (strong) allowed reflections originating from the cubic perovskite structure, extra (weak) superlattice reflections (F-spots) appear at positions of (h + 1/2, k + 1/2, l + 1/2) from the fundamental reflections. The intensity of the superstructure spot along the [1 1 1] axes varies from one crystal to another one. The existence of the F-spots clearly confirms that the ordered regions have a doubled perovskite unit cell. Fig. 4(b) and (c) shows the bright- and dark-field TEM images of the domain structures observed in the 0.25BTO–0.75BFO multiferroic ceramic sample. The dark-field TEM image was obtained using the (1 1 0) fundamental spot. As demonstrated in Fig. 4(b) and (c), wavy rhombohedral (ferroelectric) domain structures were observed in the 0.25BTO–0.75BFO multiferroic ceramics with a rhombohedral phase structure. The lengths of the domains were about 0.16 μm and their widths were about 20 nm. Furthermore, the domain walls do not seem to prefer any one set of crystallographic planes, and their waviness was ascribed to the continuous bending of the domain orientation between various equivalent directions on a length scale of 0.16 μm. Similar domain structures were reported for the bismuth and zinc-modified $Pb(Ni_{1/3}Nb_{2/3})O_3$–$PbZrO_3$–$PbTiO_3$ piezoelectric ceramics with a rhombohedral symmetry [7]. With increasing the BTO content up to 33 mol%, the phase structure of BTO–BFO multiferroic ceramics changed from rhombohedral phase to a pseudo-cubic phase, and their domain morphology exhibited a predominant intricate domain structure with fluctuating mottled contrast, as shown in Fig. 5 (a dark-field TEM image formed by the (1 0 0) diffraction spot).

4. Conclusions

Perovskite multiferroic $x$$BaTiO_3$–$(1-x)$$BiFeO_3$ solid solutions with $0.20 \leq x \leq 0.33$ were successfully prepared by the solid-state reaction. X-ray diffraction patterns demonstrated that a structural transition from rhombohedral to pseudo-cubic phase structures appeared around $x = 0.33$, and the $BaTiO_3$-doping could effectively depress the formation of impurity phase of $Bi_2Fe_4O_9$. The dielectric constants of $x$$BaTiO_3$–$(1-x)$$BiFeO_3$ solid solutions decreased with the frequency, and the degree of decrease was related to the content of $BaTiO_3$. Ferroelectric domain configurations in the multiferroic $BiFeO_3$–$BaTiO_3$ solid solutions with rhombohedral symmetry, exhibited a wavy character. The SAED patterns revealed extra (weak) superlattice reflections (F-spots) appearing at positions of (h + 1/2, k + 1/2, l + 1/2) from the fundamental reflections, indicating that the ordered regions have a doubled perovskite unit cell. In the multiferroic $BiFeO_3$–$BaTiO_3$ solid solution with pseudo-cubic phase structure, a predominant intricate domain structure with fluctuating mottled contrast was observed.

Acknowledgements

This work is supported by Natural Science Foundation of China (Grant No. 10874065), Ministry of Science and Technology of China (Grant No. 2009CB929503), and the project sponsored by the Scientific Research Foundation for the Returned Overseas Chinese Scholars, State Education Ministry.

References

[1] M. Fiebig, Revival of the magnetoelectric effect, Journal of Physics D: Applied Physics 38 (2005) R123–152.
[2] G. Catalan, J.F. Scott, Physics and applications of bismuth ferrite, Advanced Materials 21 (2009) 2463–2485.
[3] N.A. Hill, Why are there so few magnetic ferroelectrics? Journal of Physical Chemistry B 104 (2000) 6694–6709.
[4] M.M. Kumar, A. Srinivas, S.V. Suryanarayana, Structure property relations in $BiFeO_3$–$BaTiO_3$ solid solutions, Journal of Applied Physics 87 (2000) 855–861.
[5] J.S. Kim, C. Chaeon, C.H. Lee, P.W. Jang, Weak ferromagnetism in the ferroelectric $BiFeO_3$–$ReFeO_3$–$BaTiO_3$ solid solutions (Re = Dy, La), Journal of Applied Physics 96 (2004) 468–475.
[6] S.O. Leontsev, R.E. Eitel, Dielectric and piezoelectric properties in Mn-modified $(1-x)BiFeO_3$–$xBaTiO_3$ ceramics, Journal of the American Ceramic Society 92 (2009) 2957–2961.
[7] X.H. Zhu, J.M. Zhu, S.H. Zhou, Z.G. Liu, N.B. Ming, Z.Y. Meng, Ferroelectric domain structures and their morphology evolution in the $Pb(Ni_{1/3}Nb_{2/3})O_3$–$PbTiO_3$–$PbZrO_3$ piezoelectric ceramics modified by bismuth and zinc substitutions, Journal of the American Ceramic Society 91 (2008) 227–234.